

Effect of double corrugated steel plate shear wall on the seismic performance of steel moment resisting frame structure

Elyas Baboli Nezhadi, Mojtaba Labibzadeh*, Farhad Hosseinlou and Majid Khayat

Department of Civil Engineering, Faculty of Civil Engineering and Architecture, Shahid Chamran University of Ahvaz, Ahvaz, Iran

(Received March 9, 2025, Revised June 2, 2025, Accepted June 12, 2025)

Abstract. This paper presents a detailed evaluation of the performance of Double Corrugated Steel Plate Shear Walls (DCSPs) through comprehensive numerical analysis. The study is conducted in three distinct phases. The target is to determine how DCSPs would perform if it was the main lateral bearing system of a pre-designed dual system enhanced by moment frames and X-Braces. In the first phase, six numerical models were developed using Abaqus to assess the effectiveness of DCSPs compared to conventional industrial braced frames. The analysis focused on steel structures ranging from 10 to 30 stories, incorporating both DCSPs and traditional brace sections. To ensure a fair comparison, the capacities of the two systems were equalized at three different building heights. Push-over analysis revealed that DCSPs in shorter structures exhibit load-displacement capacities similar to those of braced frames, which aligns with the desired performance. However, as the building height increases, DCSPs demonstrate superior material efficiency, maintaining equivalent load-displacement capacities. In the second phase, the study examines the structural performance of DCSPs in high-rise buildings by determining the Response Modification Factor (R factor) for both systems using push-over curves. The results indicate that DCSPs achieve a higher R factor compared to braced frames despite both systems displaying nearly identical push-over curves with comparable capacities. This suggests that DCSPs offer enhanced structural performance under seismic conditions. The third phase involves a time-history analysis of two models: one with 10-story frames enhanced by braces and the other by DCSPs. Both systems were subjected to two different earthquake scenarios to evaluate base shear, drift, plastic behavior, and energy outputs. Although both systems were designed to have similar capacities, DCSPs demonstrated superior performance and greater capacity. The DCSPs are a practical option for structural enhancement compared to traditional braced frames, offering better overall efficiency and resilience in seismic events.

Keywords: braced frames; earthquake engineering; lateral enhancement; numerical simulations; push-over analysis; response modification factor; steel plate shear walls; structural engineering; time history analysis

1. Introduction

Selecting an appropriate structural system to enhance a building's resilience against natural phenomena, such as earthquakes, remains a central research topic and subject of scholarly discourse (Wang *et al.* 2018). Over time, shear walls have demonstrated their effectiveness in construction, and steel shear walls have notably shown efficiency in reducing construction costs and expediting the building process (Ghodratian-Kashan and Maleki 2021). In contrast, Corrugated Steel Plates offer distinct advantages over Flat Steel Plates when employed as a lateral resistance system, notably providing superior out-of-plane stiffness, which contributes to enhanced buckling prevention (Dai *et al.* 2018, Tong *et al.* 2020a). Despite these merits, the application of this system in high-rise buildings has not undergone thorough testing (Vaziri *et al.* 2021). DCSPs offer significant advantages not only for their structural benefits but also for their architectural applications. Due to the relatively low thickness of the sheets and the ability to create openings without compromising structural damage,

this system stands out in both structural and architectural contexts. It is particularly advantageous for use in high-rise modular structures, especially those that are prefabricated. The system's flexibility and efficiency make it a valuable option for modern construction (Deng *et al.* 2023). Seven laboratory models, scaled at 1/3, were analyzed and evaluated under cyclic loading conditions. Additionally, a finite element model of the double corrugated steel plate was developed to validate the laboratory results. The study investigated the effects of various parameters, including the depth and length of the corrugated sheets, the bolts connecting the sheets, and the material properties of the sheets (Deng *et al.* 2022). Ghodratian-Kashan and Maleki conducted a study by constructing three models at a 1/2 scale and validating them with simulated numerical models. They investigated the impact of connecting corrugated plates in a double system, as well as the effects of attaching or detaching the corrugated sheets from the frame columns (Ghodratian-Kashan and Maleki 2021). Ghodratian-Kashan and Maleki investigated the cyclic performance of a double corrugated steel shear wall system through numerical simulations using Abaqus software. The study focused on variable parameters such as the connection of the sheets to the frame members, the orientation of the sheets, the thickness of the sheets, and the width-to-height ratio of each

*Corresponding author, Ph.D., Professor,
E-mail: labibzadeh_m@scu.ac.ir

frame. These parameters were compared in terms of dissipated energy, initial stiffness, and ultimate strength to evaluate their impact on the system's overall performance (Ghodratian-Kashan and Maleki 2021). Tong and colleagues conducted both experimental and numerical studies to investigate the double corrugated steel plate shear wall system. They examined the effects of column cross-section type and sheet connections through the cyclic behavior of the system. Additionally, they studied the buckling behavior under in-plane shear forces, applying both uniform and cyclic loads to the samples to evaluate the system's performance (Tong *et al.* 2018, 2023). Researchers have investigated the shear and lateral behavior of double corrugated steel shear walls through both laboratory experiments and numerical modeling, including push-over analysis. The findings indicate that as the width-to-height ratio decreases, the shear resistance increases, largely due to the near-complete yielding of the shear wall material. Additionally, increasing the number of bolts connecting the two sheets has a positive impact on the ultimate shear strength of the system, particularly in cases with wider span (Tong *et al.* 2020a, b). Feng Ki Guo conducted a numerical investigation into the effects of openings in steel corrugated shear wall systems, particularly in modular high-rise structures. The study examined various types of openings and their impact on structural performance. To advance the research, time history analysis was utilized, where the acceleration data from real earthquakes were scaled and applied to the structure. The authors specifically tested several spans of a 15-story prefabricated structure, equipped with shear wall systems containing openings, under the acceleration of the El Centro earthquake (Jing *et al.* 2023). Additionally, damage indices for corrugated steel plate shear walls were established, and data from 12 far-field earthquakes were analyzed, ultimately resulting in a fragility analysis (Dadmanesh and Mofid 2024). Research conducted by Jeffrey W. Berman, Oguz C. Celik, and Michel Bruneau aimed to compare corrugated steel plate shear walls with common bracing systems (Berman *et al.* 2005). Additionally, Mehran Zeynalian and H.R. Ronagh utilized Push-Over analysis and a capacity-equivalent method for structural system replacement in their numerical simulations. This approach has laid the foundation for the design and comparison conducted in the subsequent research presented in this paper (Zeynalian and Ronagh 2011).

Furthermore, the elastic buckling response was analyzed, leading to the development of a stability design approach for the double corrugated steel plate shear walls subjected to combined shear and compression loads (Wen *et al.* 2024). The configuration of corrugated plates within frames was examined as a design parameter, with 33 specimens analyzed using FE analysis in Abaqus software (Noruzi and Jalaeefar 2024). Despite their potential, double corrugated steel plate shear walls have lacked a practical and reliable lateral design methodology. To bridge this gap, a machine learning-based study was conducted using a database of numerically simulated and experimental samples. These samples underwent push-over analysis to assess shear strength, resulting in the proposal of a design

model and equations to accurately predict buckling behavior and ultimate shear capacity (Baboli Nezhadi *et al.* 2024). Another method was introduced to calculate the load-bearing capacity of corrugated steel plate shear walls under combined shear and axial forces (Li *et al.* 2025). Additionally, a recent study focused on the compatibility of strength and stiffness between the main plates and boundary columns (Yang *et al.* 2025).

Chao Dou and his colleagues comprehensively investigated the buckling behavior of trapezoidal corrugated steel plates. Using finite element analysis, they validated various buckling modes including local, global, and interactive buckling (Dou *et al.* 2025). Additionally, the performance of corrugated steel plate shear walls, particularly in large width-to-height ratio frames was enhanced, through two innovative approaches, firstly, combining corrugated plates with flat steel plates (Dou *et al.* 2023), and secondly, implementing grid-reinforced enhancement techniques (Chao *et al.* 2024).

Researchers have extensively studied tall structural systems, with a focus on mitigating concrete column shortening—a critical design challenge in high-rises. An early work demonstrated that material properties (e.g., aggregate elasticity and cement hardening speed) significantly influence axial shortening, while environmental factors like temperature play a secondary role (Ali *et al.* 2017). To improve prediction accuracy during construction, an analytical correction method using limited field measurements was proposed, showing that error reduction is most effective in later construction stages (Song and Kim 2022). Expanding on this, a column-grouping approach was introduced to normalize shortening values across all floors, minimizing prediction errors even at unmeasured points (Song and Kim 2020). Together, these studies highlight the interplay of material science and computational tools in tall structures assessment. Recent studies have advanced tall building shear wall systems (Zhang *et al.* 2021), post-earthquake damage assessment methods for flexural-dominated walls (Komarizadehasl and Khanmohammadi 2021), and performance enhancement using fiber-reinforced concrete (PVA fibers showing superior crack control). These developments address critical seismic needs in high-rise design.

The double corrugated steel plate shear wall system offers several advantages, including enhanced shear resistance, reinforced buckling performance, material efficiency, and flexibility in design, making it a promising solution for structural enhancement against earthquakes. Despite these benefits, there is a need for further research to fully understand and optimize the performance of this system in taller buildings. Comparing this innovative system with more conventional solutions, such as bracing frames, will provide valuable insights and help determine the most effective strategies for improving the structural resilience and efficiency of high-rise constructions.

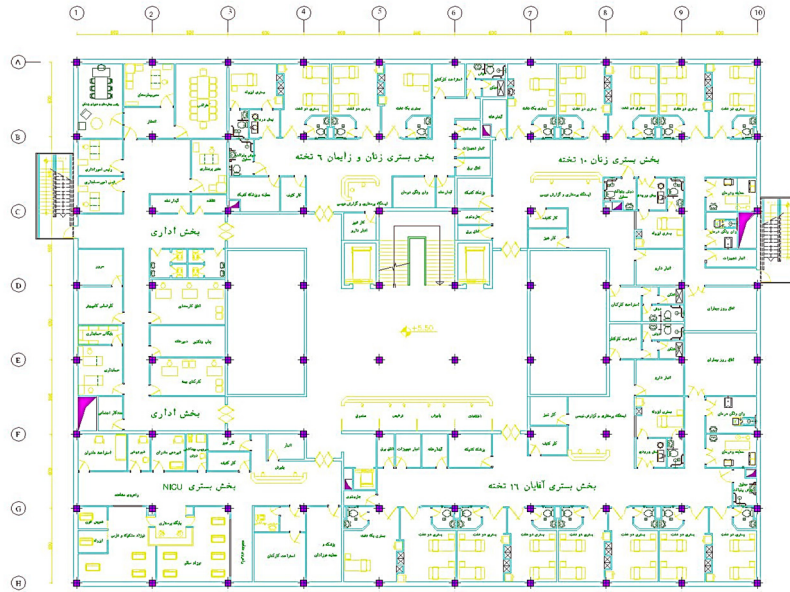


Fig. 1 Case study plan

2. Methodology: Level 1

2.1 Frame design: Level 2

To investigate the effect of increasing building height, three structures with 10, 20, and 30 stories were modeled using ETABS software and designed in accordance with AISC 360 and ASCE 7 regulations (ANSI/AISC 360-16 2016). To ensure the structural conditions closely align with

Each story has a height of 3.2 meters, and the span width is 6 meters. The selected structure was modeled in three dimensions and reinforced with a steel bracing lateral bearing system in both directions, resulting in a dual system consisting of moment frames with X-bracing. For further two-dimensional analysis, the critical frame was selected.

Given that there is no optimal design method available for the interaction between moment frames and double corrugated shear walls, the purpose of this chapter is to eventually replace the bracing system with the double

Table 1 Frame design outputs

Structure	RTB			IPG		
	Dimensions	Thickness	Flange width	Flange thickness	Web geight	Web thickness
10 Story	500 × 500 mm ²	35 mm	200 mm	20 mm	375 mm	8 mm
20 Story	600 × 600 mm ²	40 mm	250 mm	35 mm	375 mm	15 mm
30 Story	600 × 600 mm ²	40 mm	250 mm	35 mm	375 mm	15 mm

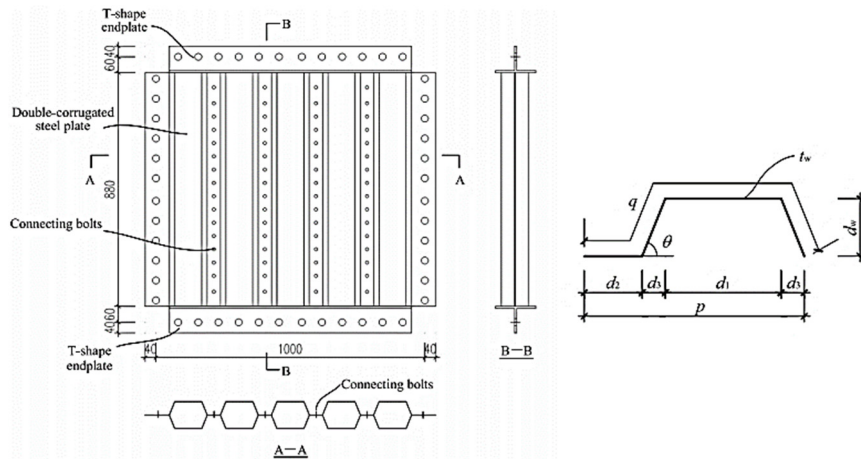


Fig. 2 Configuration of the corrugated plate (Dong *et al.* 2022)

Table 2 Geometric properties of the samples (Deng *et al.* 2022)

Model	Configuration	Sm (mm)	Nb	d1 (mm)	d2 (mm)	d3 (mm)	Dw (mm)	Tw (mm)	Steel grade
L-SCSP1	Single-corrugated	/	/	100	50	20	50	1	Q235B
L-DCSP1	Double-corrugated	200	1	100	50	20	50	1	Q235B
L-DCSP2	Double-corrugated	100	1	100	50	20	50	1	Q235B
L-DCSP3	Double-corrugated	50	1	100	50	20	50	1	Q235B
L-DCSP4	Double-corrugated	50	2	100	50	20	50	1	Q235B
L-DGSP1	Double-corrugated	100	1	50	50	20	10	1	Q345B
L-DGSP2	Double-corrugated	100	1	70	50	20	10	1	Q345B

Table 3 Steel material properties (Deng *et al.* 2022)

Group No.	Specimen label	Steel grade	f_y (mpa)	f_u (mpa)	E_s (mpa)	ϵ_u
1	L-SCSP1	Q235B	176.7	282.2	195000	0.217
2	L-DCSP1 ~ L-DCSP4	Q235B	198.1	323.8	197000	0.201
3	L-GCSP1, L-GCSP2	Q345B	447.9	547.7	236000	0.184

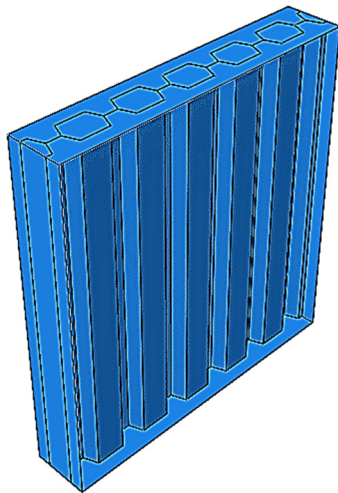
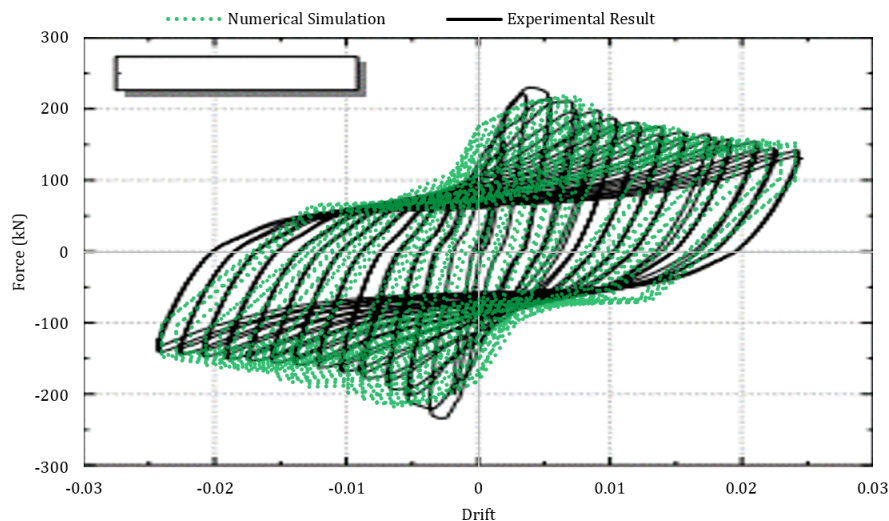


Fig. 3 Assembled models in abaqus

corrugated shear wall system. This replacement allows for a valid comparison between the two systems while ensuring that the original frame design remains compliant with design standards. The final design for the critical frame includes Rectangular Tube Box (RTB) columns, I-Wide Flange Plate Girder (IPG) beams, and bracing sections made from double channels (Table 1).

2.2 Verification: Level 2

In the current research, the study conducted by Ren Deng (Deng *et al.* 2022) has been validated. To achieve this, a double corrugated steel shear wall, previously subjected to experimental analysis, was selected and modeled using Abaqus software. The hysteresis curve of the model was verified through cyclic analysis. The sample consists of two corrugated sheets bolted together, which were tested within a pinned frame, meaning the stiffness of the frames was not

Fig. 4 Comparison of experimental and numerical hysteresis curves (Deng *et al.* 2022)

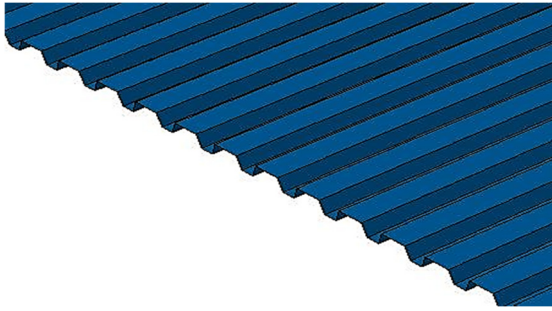


Fig. 5 Cross-section of the corrugated steel plate

Table 4 Material properties used in frame design

Elasticity module (E)	Poisson ratio (ν)	Yielding stress (f_y)	Ultimate stress (f_u)	Ultimate strain (ϵ_u)
200000 mpa	0.3	300 mpa	470 mpa	0.15

considered. The specifications of the samples and the material properties used in the study are detailed in Tables 2, 3, and Fig. 2.

Numerical modeling for the L-DCSP2 sample (Table 2) was carried out in Abaqus. In the laboratory, the supporting frame did not contribute to the lateral load-bearing capacity of the shear wall plates and the shear wall was under pure

shear load. To replicate this in the software, four rigid plates were used to model the supporting frame, with the shear wall pinned to them (Fig. 3). This approach ensures that the system’s behavior in the software accurately reflects its real-world performance.

The cyclic curves from the numerical model are compared with the experimental results in Fig. 4, demonstrating consistency between the two. The detailed process of numerical modeling is discussed in the following section.

2.3 Numerical Simulation: Level 2

In this chapter, the objective is to briefly describe the modeling details within each module using Abaqus. All components, including frame sections (beams and columns), bracing sections, and shear wall sheets, are modeled as deformable shell parts (Fig. 5).

The material properties of the steel are divided into two categories. The properties related to the beams, columns, and braces are derived from the structural design in ETABS (Table 4). However, the material properties of the shear wall sheets were verified and finalized during the validation process (Table 2).

The sections were assembled and connected part by part using Tie Constraints, which included beam-to-column connections as well as connections of the lateral systems

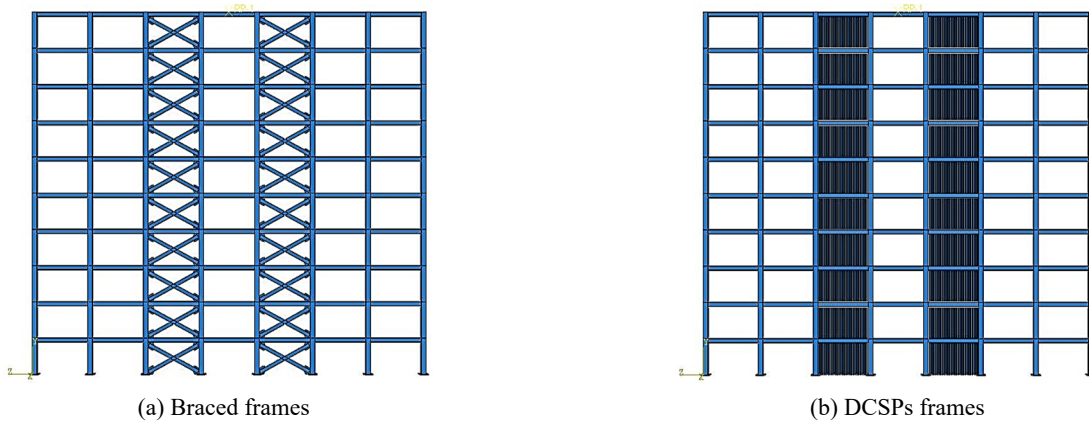


Fig. 6 Features of 10-story models

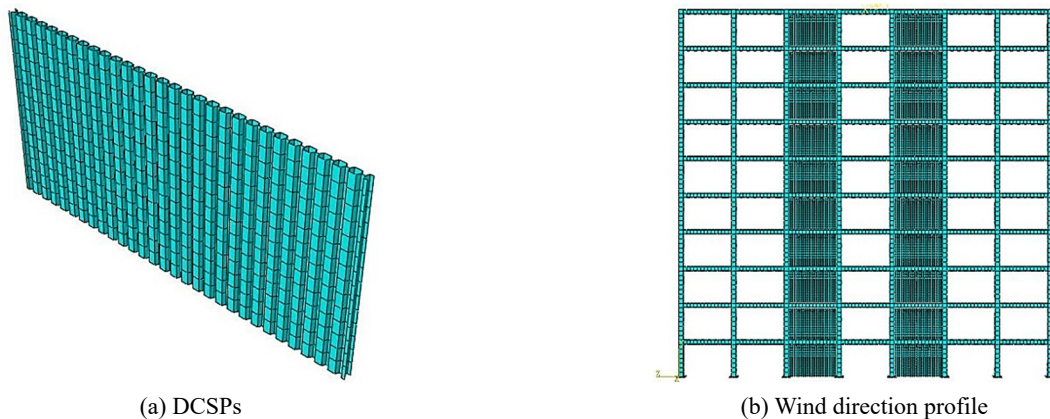


Fig. 7 Meshing details

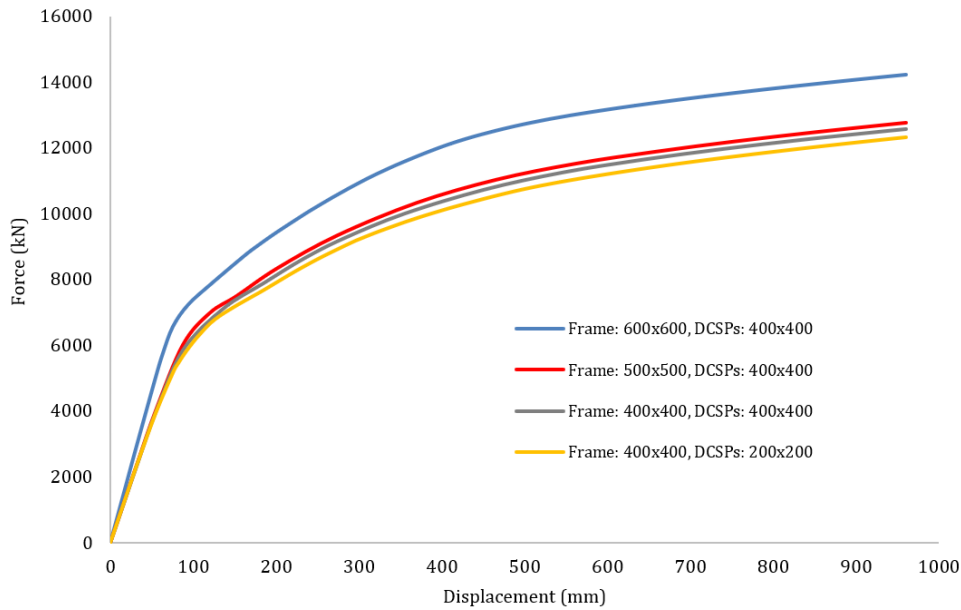


Fig. 8 Results of mesh sensitivity analysis

to the main frame. Each lateral system (DCSPs and Braces) was connected as specific parts to form the double corrugated shear wall, which consists of two separate corrugated walls and bracing sections, which consist of two separate channels duplicated throughout all stories. Frame elements were designated as Master Elements, while Braces and DCSPs were designated as Slave Elements for interaction constraints (Fig. 6).

The size and type of mesh significantly influence the accuracy of the analysis and its time optimization. In this research, the S4R element type was used. The mesh size was determined through mesh sensitivity analysis (Fig. 7). To identify the optimal mesh size for the models, Push-Over analysis was conducted on 10-story samples. Naturally, increasing the number of stories while maintaining a constant mesh size ensures reliability.

Ultimately, elements with a 400 mm mesh size were used for the Master Elements (Frames) and a 200 mm mesh size for the Slave Elements (DCSPs) (Fig. 8). As shown in the figure, the mesh dimensions were gradually refined, and the analysis was repeated until convergence of the analysis outputs was achieved.

The frames were fixed at the base plates, with constraints applied to prevent out-of-plane movement, including both translational and rotational degrees of freedom so the analysis will be done in the plane and two dimensions. To apply the ultimate push load, the top of the last story was coupled to a reference point that carried the applied displacement.

2.4 Equivalence of Models: Level 2

The objective of this section is to replace the bracing system with Double Corrugated Steel Plate Shear Walls (DCSPs) to evaluate their impact on the structural performance and response. Since the DCSPs system is not included in standard design codes, and a specific response modification factor has not been assigned to it, it is essential

to compare the performance of a frame reinforced with an X-bracing system to the same frame with an equivalent DCSPs system.

The replacement criterion is based on the amount of material required for the DCSPs to achieve the same capacity as the bracing system in structures of 10, 20, and 30 stories. As the number of stories increases, the frame elements, brace sections, and DCSPs sections will be adjusted. This approach allows for a material ratio comparison, providing valuable insights into more efficient lateral load-bearing systems.

To equate a DCSPs system with an X-braced section, the equal capacity method is used, which has been applied in previous research (Zeynalian and Ronagh 2011). In this method, the designed structure with the bracing system undergoes displacement-controlled analysis (Push-Over). The new system (DCSPs) then replaces the existing bracing system in the same frame, followed by a new analysis of the modified structure. The analysis continues by iteratively adjusting the properties of the DCSPs sheets until they achieve a capacity equivalent to the designed bracing system. Once the two structures demonstrate equivalent capacity, it can be asserted that the interaction between the designed moment frame and the DCSPs is comparable to that of the moment frame with the bracing system, confirming the frame's suitability for interaction with DCSPs as a lateral load-bearing system.

The target displacement for Push-Over analysis was obtained from FEMA 450, assuming that Seismic Group II maximum allowable drift governs the design presenting in Eq. (1) (Building Seismic Safety Council 2003)

$$U = 0.02 \times h \quad (1)$$

U represents target displacement and h stands for total structure height. The target displacement for the 10-story models is 640 mm, with 1280 mm and 1920 mm for the 20-story and 30-story structures, respectively.

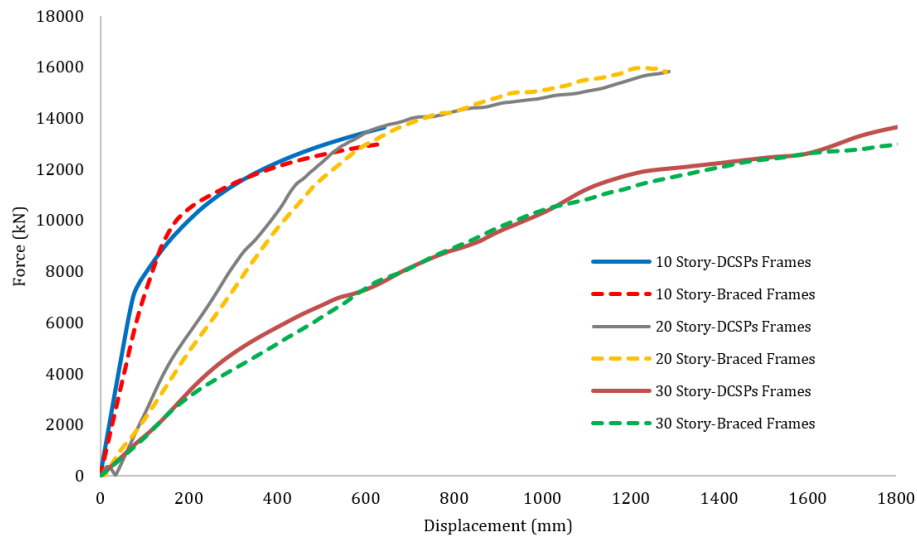


Fig. 9 Equalized pushover curves for various lateral systems

Table 5 Section details of lateral resistance systems

Model	Brace section (Tube)		Corrugated plate	
	Dimensions	Thickness		Thickness
		Web	Flange	
10 Story	$320 \times 210 \text{ mm}^2$	14 mm	16 mm	5 mm
20 Story	$350 \times 210 \text{ mm}^2$	16 mm	18 mm	5 mm
30 Story	$380 \times 220 \text{ mm}^2$	16 mm	18 mm	5 mm

After modeling two types of moment frames with different lateral load-bearing systems (braces and walls), and through several iterations, the characterization of the sheets connected to the moment frame, which achieved a capacity equivalent to the designed dual bracing system, was finalized. The mechanical and geometric characteristics of the sheets were confirmed and finalized through verification (Table 2). Therefore, the only sheet characteristic that could be modified to match the capacity of the designed bracing structure was the sheet thickness. The resulting capacity curves are shown in (Fig. 9).

Efforts were made to bring the Push-Over curves of both structural systems close together. Since the predesigned dual system (moment frame with X-brace) could not be altered, as it was the basis for this research, the only parameter that could be adjusted was the thickness of the DCSPs. Through trial and error, it was observed that a 5 mm corrugated steel plate, which would be doubled to 10 mm in the DCSPs, achieved nearly the same load displacement capacity as the predesigned system enhanced with brace frames.

The final equalized lateral bearing systems are reported in (Table 5). It is noteworthy that the geometric configuration of the corrugated plates is discussed and

verified in Chapter 2.2 and now both systems are well designed and ready for further analysis and comparison.

2.5 Scaling earthquake accelerations: Level 2

The time history analysis plays a critical role in evaluating the dynamic response of the structural model under real earthquake conditions. This method tests the model by subjecting it to the recorded acceleration data of actual seismic events, allowing for a detailed comparison of various structural outputs. For this study, two notable earthquakes, the Chi-Chi (Taiwan 1999) and Hector Mine (California 1999) events, were selected due to their significant magnitudes and well-documented ground motions.

The process began by scaling the recorded accelerations of these earthquakes to match the design criteria of the structure under analysis. Scaling ensures that the intensity of the seismic input is appropriate for the specific model, which helps in maintaining a consistent basis for comparison across different structural configurations. The square root of the sum of the squares (SRSS) method was employed to compute the resultant accelerations from the earthquake records. These values were then compared against the design spectrum to verify that the selected earthquakes were well-suited for the model under consideration. This validation step is essential, as it confirms that the selected seismic events will adequately challenge the structure and provide meaningful results for assessing its performance under real-world conditions (Figs. 10, 11).

Once the earthquake accelerations were appropriately scaled and validated, the next step involved applying these ground motions to the base of the structures in the form of time-varying acceleration inputs. This approach creates the actual seismic impact that would occur during an earthquake, allowing the analysis to capture the structural response in terms of base shear, inter-story drift, and energy outputs.

The time history analysis offers a comprehensive

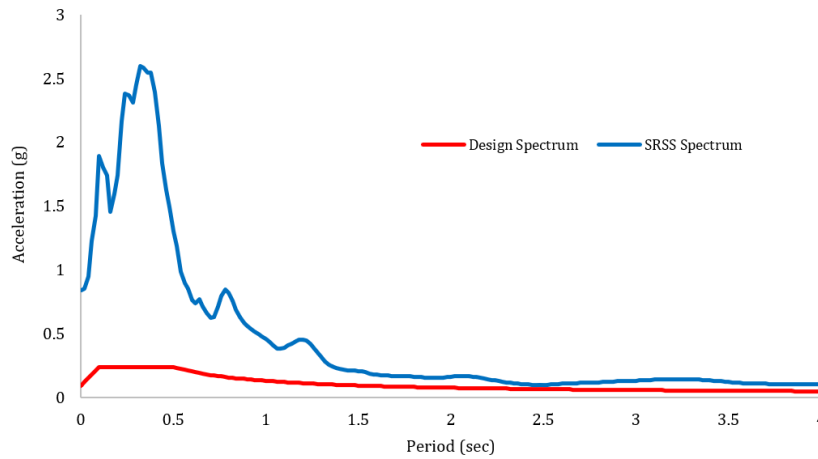


Fig. 10 Comparison of the design spectrum with the Chi-Chi SRSS Spectrum

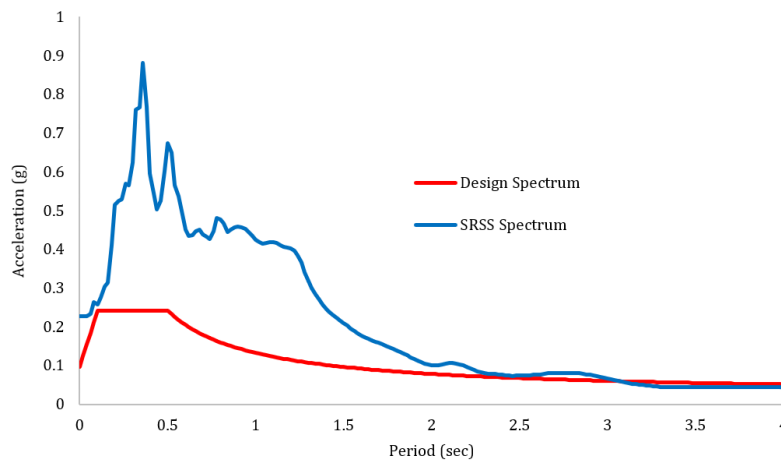


Fig. 11 Comparison of the design spectrum with the Hector Mine SRSS Spectrum

understanding of how the structure performs dynamically under varying seismic forces, highlighting potential vulnerabilities or strengths that might not be evident in static or simplified analyses. By analyzing the structural response to these two earthquakes, the study provides valuable insights into the effectiveness of the double corrugated shear wall system in comparison to the traditional braced. This analysis ultimately helps determine whether the proposed system can offer enhanced performance and safety in seismic-prone regions.

3. Results: Level 1

3.1 Push over: Level 2

3.1.1 Material efficiency: Level 3

Interesting results emerged from the analysis outputs. The 10-floor structures served as the baseline for comparison with the taller models. In the predesigned Braced Frames, the 20 and 30-floor models showed an increase in steel material volume by 11.2% and 17.1%, respectively, compared to the 10-floor Braced model. However, for the 20 and 30-floor structures reinforced with DCSPs, the material volume

remained nearly equal to that of the 10-floor DCSPs model (Fig. 12). The slight reduction in DCSPs volume is attributed to the increase in beam and column dimensions during the frame design process (Table 1). These volumes are derived from the design outputs listed in Table 5.

Moreover, the observation of ultimate stresses from the analysis provides additional insights. The final stress levels in structures reinforced with the double corrugated shear wall (DCSPs) system were higher compared to those with bracing systems (Fig. 13). However, the greater amount of material in the DCSPs system contributed to better stress distribution. The larger contact surface between the shear wall sheets and the surrounding frame helps distribute stress more evenly, thereby protecting the frame elements from potential fracture. In contrast, the bracing gusset plates tend to stress concentration in localized areas, increasing the risk of failure. This improved stress distribution highlights one of the key advantages of the DCSPs system over traditional bracing.

3.1.2 R Factor: Level 3

The Response Modification Coefficient (R) for 10, 20, and 30-story structures reinforced with both bracing systems and double corrugated steel plate shear walls

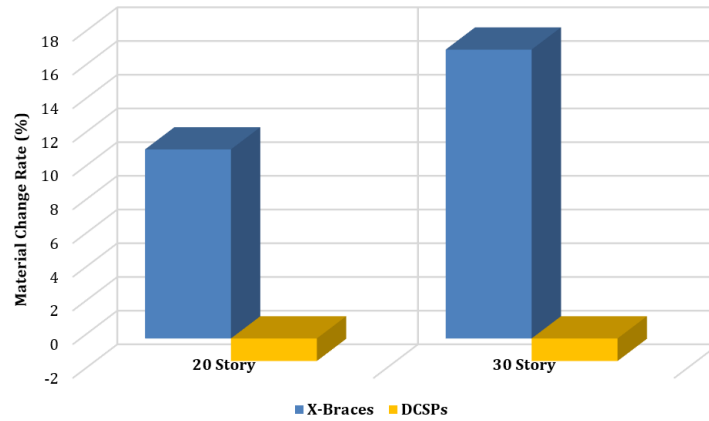


Fig. 12 Material change rate compared to 10-story models for the two systems under study

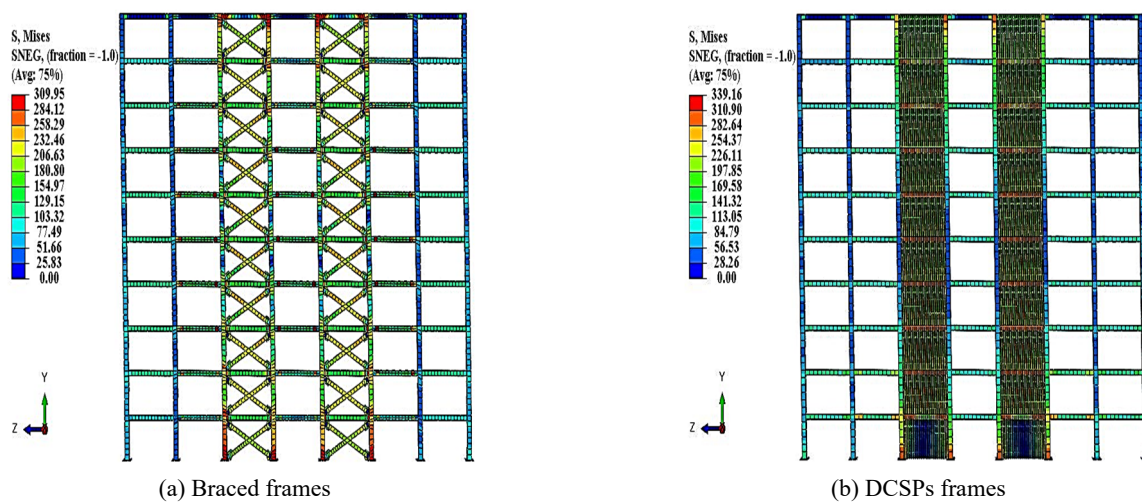


Fig. 13 von Mises stress values

(DCSPs) has been extracted through detailed analysis. The bilinearization process of the Push-Over capacity curve was conducted following the ATC-19 guidelines and the Priestly-Pauli method (Rojahn *et al.* 1995, Paulay and Priestley 1992, Federal Emergency Management Agency 2003).

Bilinearization involves simplifying a pushover curve into a bilinear representation, comprising an elastic segment and a plastic segment. The elastic segment reflects the structure’s initial stiffness, whereas the plastic segment captures its post-yield behavior. The primary objective of bilinearization is to streamline the computation of critical seismic performance metrics, such as the response modification factor (R), which are crucial for assessing a structure’s ability to resist seismic forces. This simplified approach is extensively employed in performance-based seismic design to analyze and evaluate the nonlinear response of structures.

Figs. 14 and 15 illustrate the bilinearization process for the 10-story structures, with the capacity curve from the Push-Over analysis displayed as a representative sample. Additionally, Table 6 presents the R coefficient for all six analyzed structures.

Upon reviewing the results, it becomes evident that

Table 6 R coefficients for various models

Structure type	10 stories	20 stories	30 stories
DCSPs frames	$R_u = 5.06$	$R_u = 3.52$	$R_u = 3.53$
Braced frames	$R_u = 3.16$	$R_u = 2.44$	$R_u = 2.49$

while the capacity curves for both systems show similar ultimate capacities, the behavior coefficient (R) and ductility of the DCSPs system are superior to those of the bracing system. This indicates improved performance under seismic loads in the shear wall system. The R coefficient is higher for the double corrugated system compared to the bracing system. However, it is important to note that as the height of the structure increases and the moment frame’s contribution becomes more pronounced, the R coefficient gradually decreases. As a result, the changes in the R coefficient become less significant with the increase in building height for each specific lateral system.

3.2 Time history analysis: Level 2

To better understand the detailed performance of double corrugated shear wall systems (DCSPs), a nonlinear

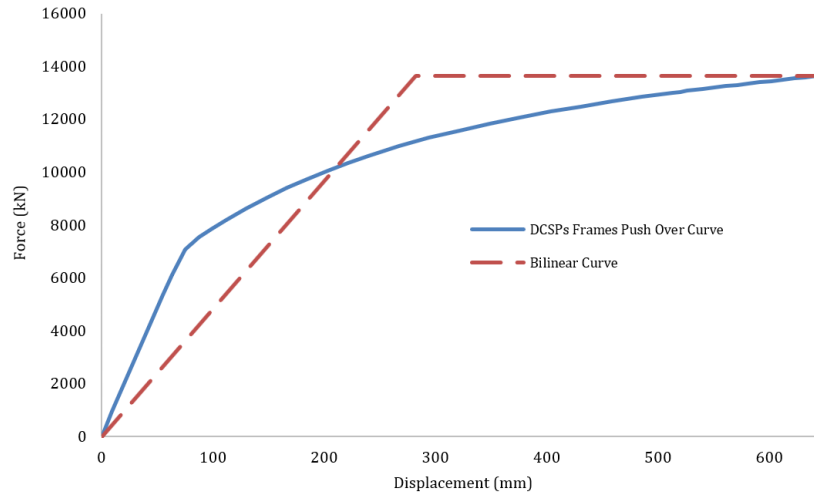


Fig. 14 Bilinearization process for DCSPs frames capacity curve

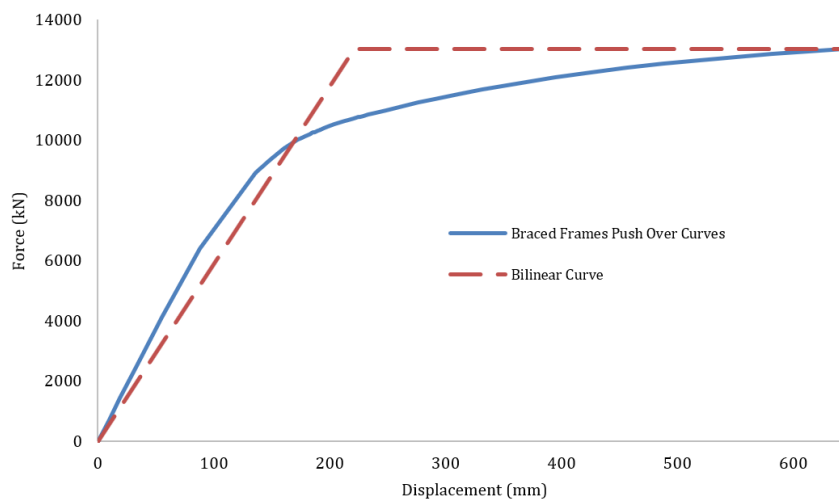


Fig. 15 Bilinearization process for braced frames capacity curve

dynamic time-history analysis was conducted. This approach, consistent with methodologies employed in previous studies (Dey and Alam 2024, Habibi *et al.* 2020, Ouzandja *et al.* 2025), compared the seismic performance of 10-story DCSPs with conventional 10-story X-bracing systems. The comparison criterion used was the similarity of the capacity curves between the two systems, ensuring that both systems were assessed under comparable conditions.

The outputs examined in this analysis included: Von Mises stress, equivalent plastic strain, total internal energy, strain energy, base shear, and story drift. These parameters were chosen due to their frequent use in similar comparisons, where time history analysis is employed to evaluate the dynamic response of structures (Guo *et al.* 2023, Etedali *et al.* 2019, Jing *et al.* 2023). This comprehensive set of metrics allows for an in-depth evaluation of the behavior of both systems under seismic loading, providing valuable insights into their structural performance.

3.2.1 Visual outputs: Level 3

3.2.1.1 von Mises Stress: Level 4

By examining the ultimate stresses generated in the models, it is evident that the final stresses in structures reinforced with a double corrugated shear wall (DCSPs) are lower and more controlled compared to those observed in the Push-Over analysis (Figs. 16-19).

A key advantage of the DCSPs system is its ability to concentrate maximum stresses within the wall sheets themselves. This means that the system effectively protects the structural frames, which serves as proof of the successful application of the equal capacity method in its design.

As a result, it can be confidently stated that the DCSPs system plays a primary role in structural reinforcement by absorbing seismic stresses, thereby shielding critical structural elements such as columns from damage. This stress distribution capability enhances the overall performance and resilience of the structure, particularly in the face of seismic events.

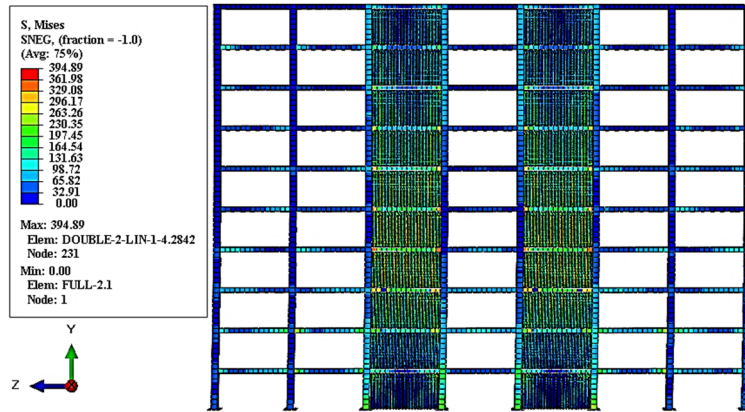


Fig. 16 von Mises stress values in the DCSPs frames under Chi-Chi Accelerations

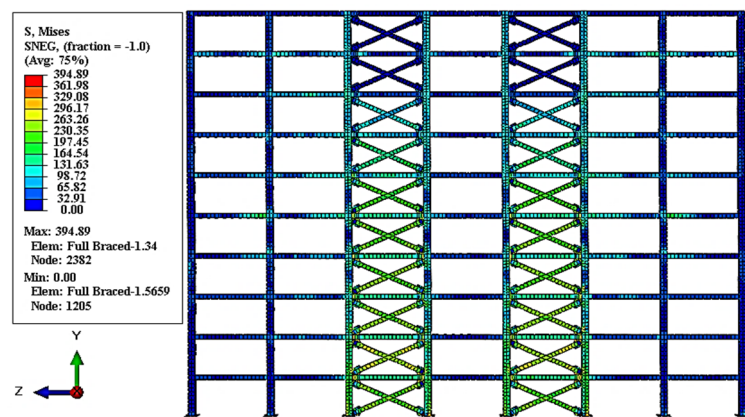


Fig. 17 von Mises stress values in the braced frames under Chi-Chi Accelerations

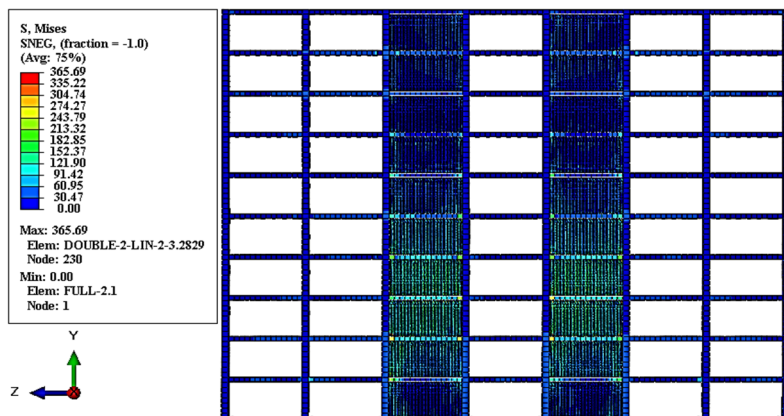


Fig. 18 von Mises stress values in the DCSPs frames under Hector Mine Accelerations

3.2.1.1 Equivalent plastic strain: Level 4

The Equivalent Plastic Strain (PEEQ) is a dimensionless number, making it an appropriate metric for comparing two structural systems. When the PEEQ value exceeds zero, it indicates that the structure has entered the plastic phase, signifying the formation of plastic hinges (Figs. 20-23).

Upon analyzing the strains generated in the structures, it can be concluded that both the braced system and the

double corrugated shear wall system exhibit good plastic behavior, with performance levels close to each other.

However, the structure reinforced with the shear wall system demonstrates slightly superior plastic behavior. This suggests that a larger volume of material in the shear wall system undergoes yielding, resulting in more efficient and economical structural performance (Table 7).

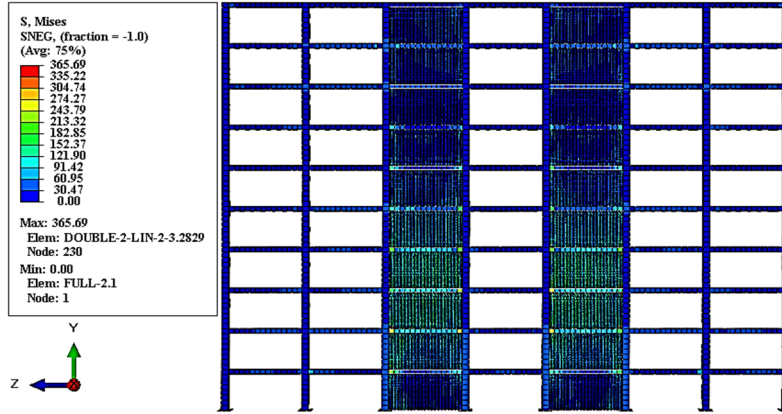


Fig. 19 von Mises stress values in the DCSPs frames under Hector Mine Accelerations

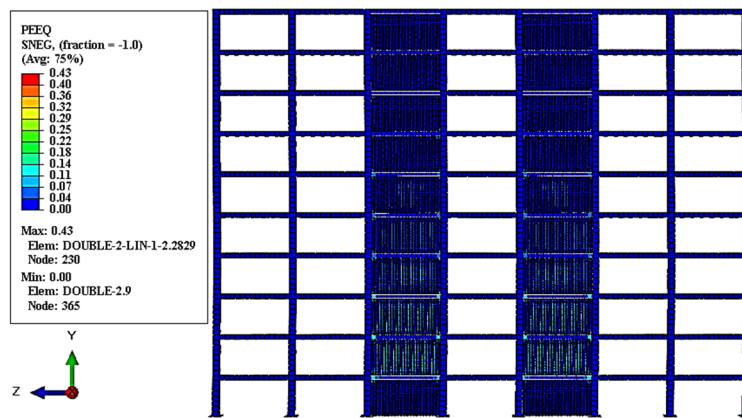


Fig. 20 PEEQ values in the DCSPs frames under Chi-Chi Accelerations

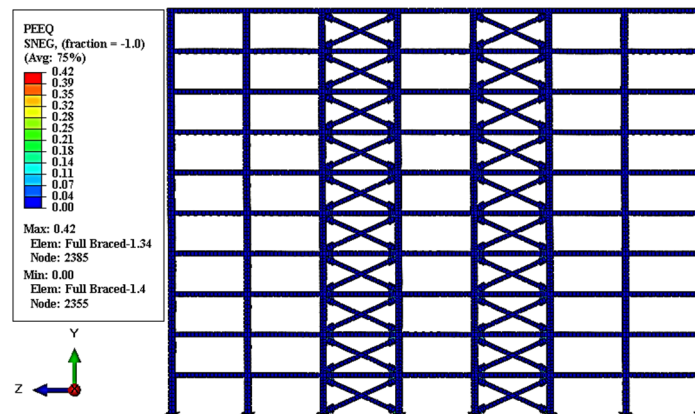


Fig. 21 PEEQ values in the braced frames under Chi-Chi Accelerations

Table 7 Maximum PEEQ generated in the two systems under study

Model	Maximum equivalent plastic strain	
	Under Chi-Chi Accelerations	Under Hector Mine Accelerations
DCSPs frames	0.43	0.19
Braced frames	0.42	0.18

3.2.2 Parametric outputs: Level 3

3.2.2.1 Internal energy: Level 4

The All Internal Energy (ALLIE) represents the total energy absorbed by the structure during seismic activity. The ALLIE values for both systems during the earthquake simulations are presented in Figs. 24-25.

If the primary design goal is to maximize energy absorption and enhance failure resistance, a structural

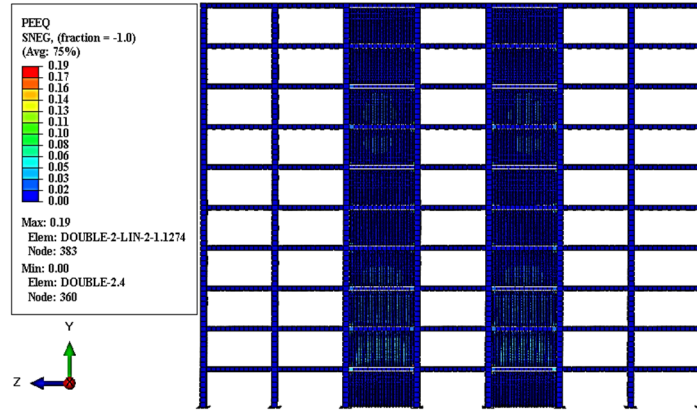


Fig. 22 PEEQ values in the DCSPs frames under Hector Mine Accelerations

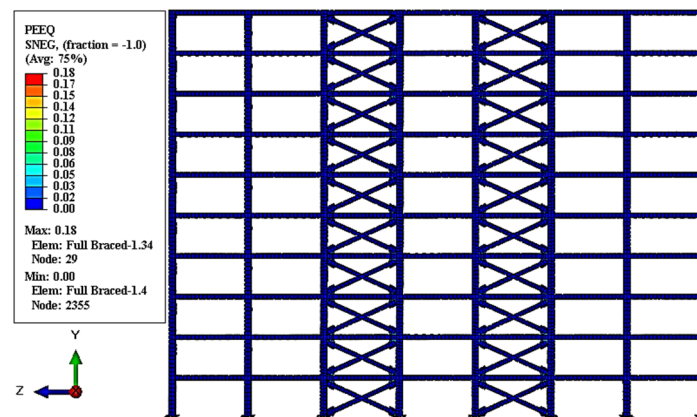


Fig. 23 PEEQ values in the braced frames under Hector Mine Accelerations

system that exhibits higher input energy is more advantageous. Based on this criterion and the observations in Figs. 24 and 25, the double corrugated steel plate shear wall (DCSPs) system proves to be the better option. During the selected earthquake simulations, the DCSPs consistently achieve higher ALLIE values throughout the seismic event.

Furthermore, the ultimate ALLIE before the transition to free vibration—where internal energy ceases to increase and the curve flattens—is significantly higher in the DCSPs system. This suggests that DCSPs are more effective in

energy absorption and may provide greater structural resilience during earthquakes.

3.2.2.2 Strain energy: Level 4

The All Strain Energy (ALLSE) represents the energy stored in the structure due to elastic, reversible deformations. The ALLSE values for both the braced system and the double corrugated shear wall system (DCSPs) during the earthquake simulations are shown in Figs. 26-27.

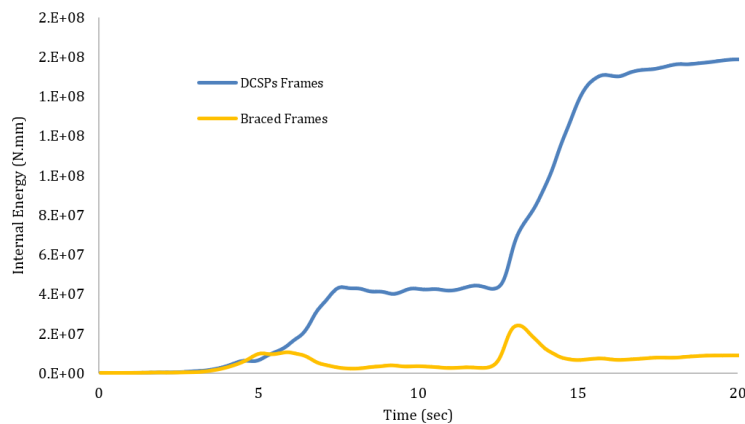


Fig. 24 Total internal energy for various lateral systems under Chi-Chi Accelerations

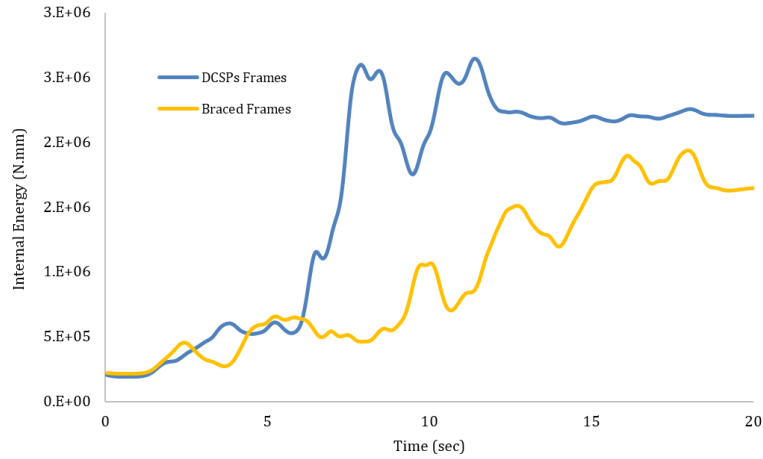


Fig. 25 Total internal energy for various lateral systems under Hector Mine Accelerations

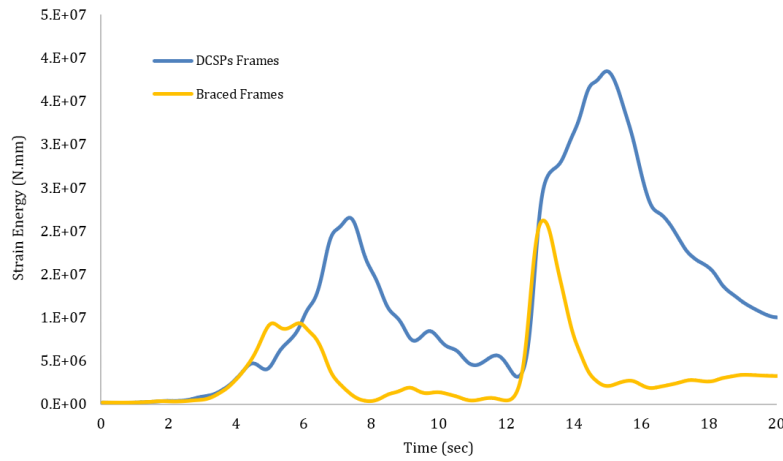


Fig. 26 Total strain energy for various lateral systems under Chi-Chi Accelerations

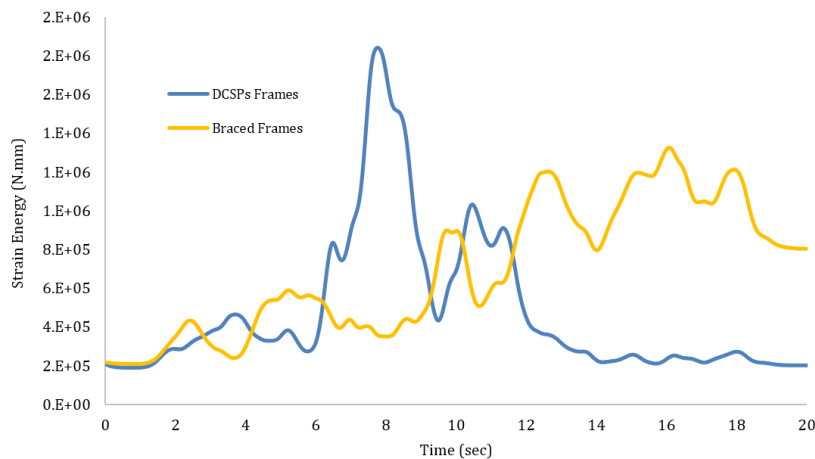


Fig. 27 Total strain energy for various lateral systems under Hector Mine Accelerations

If the design objective is stability and efficiency in bearing dynamic loads without transitioning into the plastic zone, a system that stores more strain energy would be preferred. Given the superior plastic behavior of the DCSPs system, it is clear that the bracing system exhibits more elastic behavior. However, the elastic performance of the

double corrugated shear wall system remains significant.

Notably, during the more intense Chi-Chi earthquake, the DCSPs system demonstrated greater elastic resilience. Similarly, during the intense phase of the Hector Mine earthquake, the DCSPs system also exhibited enhanced elastic behavior, indicating that it can maintain stability

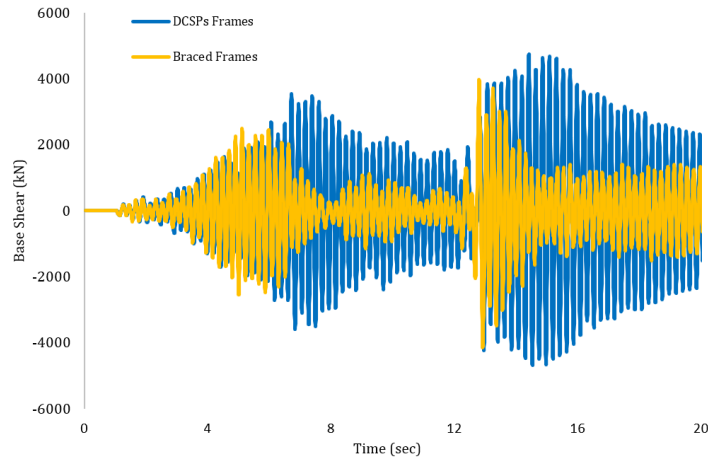


Fig. 28 Base shear response of both lateral systems under Chi-Chi Accelerations

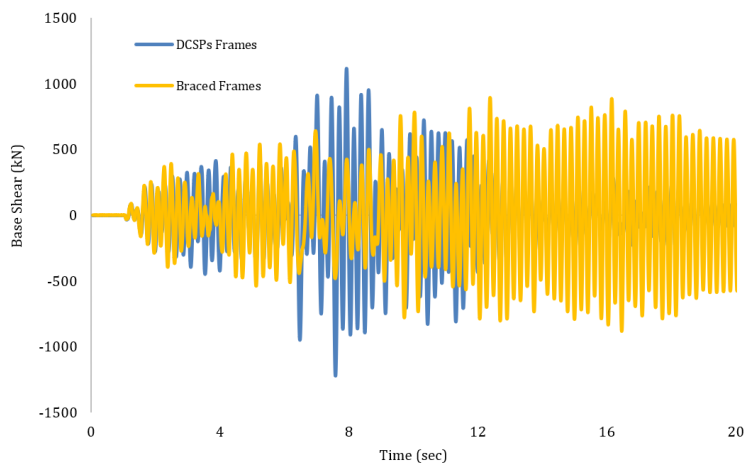


Fig. 29 Base shear response of both lateral systems under Hector Mine Accelerations

under extreme conditions while still offering a high level of performance.

3.2.2.3 Base shear: Level 4

Base shear is a key parameter for assessing the capacity of structures equipped with different lateral load-resisting systems. The base shear values for both the braced system and the double corrugated shear wall system (DCSPs) during earthquake simulations are depicted in Figs. 28 and 29.

The base shear results largely indicate a stiffer response from the double corrugated shear wall system. Consequently, it can be concluded that although the DCSPs system demonstrated nearly equal capacity to the braced system in the Push-Over analysis, it significantly outperforms the braced system when subjected to actual earthquake accelerations. The superior base shear capacity observed in dynamic analysis highlights the enhanced performance of the DCSPs system under seismic loads, showcasing its ability to resist larger forces more effectively than the bracing system.

3.2.2.4 Drift: Level 4

Structural relative drift is a key indicator of the ductility and flexibility of structural systems. The story drift and

mean drift values for both the braced system and the double corrugated shear wall system (DCSPs) during earthquake simulations are shown in Fig. 30.

The mean relative drift (Fig. 30(c)), averaged from the outputs of the two selected earthquakes in both systems, remains within acceptable and controlled limits. However, the higher mean relative drift observed in structures reinforced with shear walls indicates the greater ductility of the DCSPs system. This increased drift supports the conclusion that the DCSPs system has a higher response modification coefficient (R), confirming its superior capacity to absorb and dissipate seismic energy. Further highlighting its flexibility compared to the bracing system.

4. Conclusions

The DCSPs system demonstrates several beneficial points worth highlighting:

- **Capacity in Tall Structures:** The system shows remarkable capacity in tall structures, with no significant increase in material volume required to achieve the same capacity as bracing systems, even as the number of floors increases.

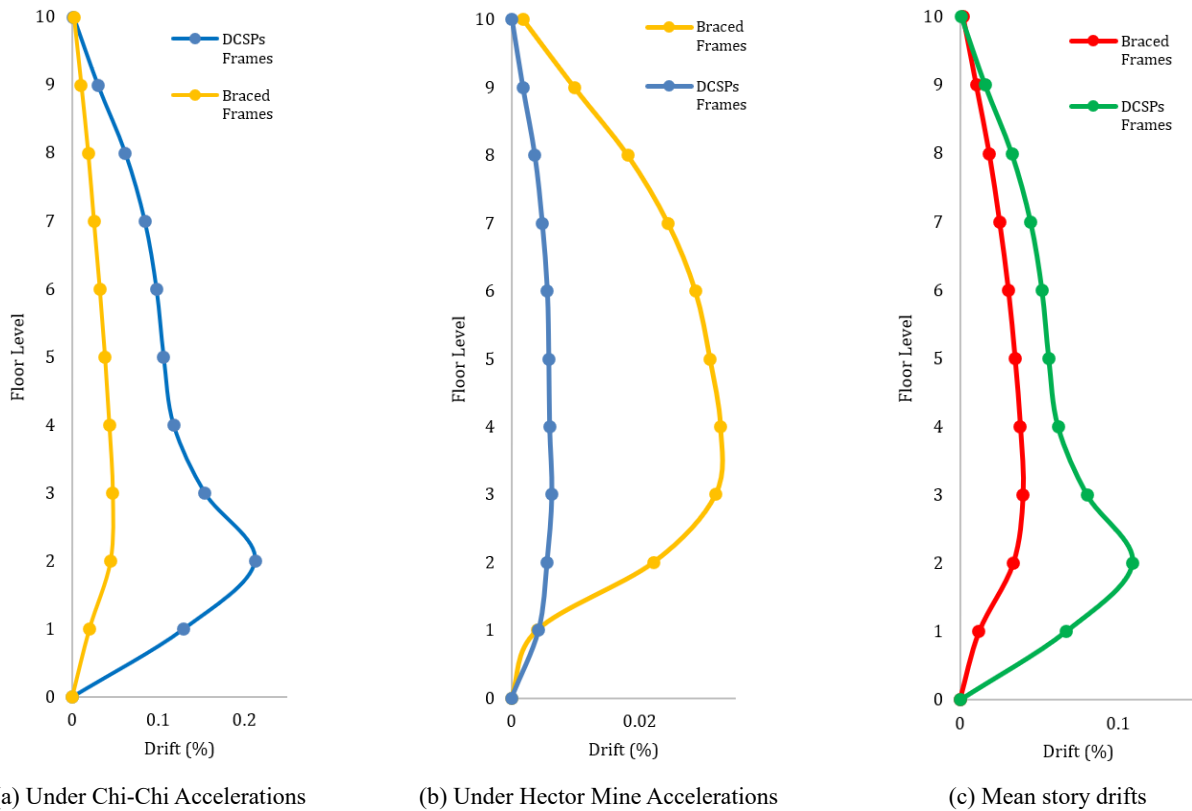


Fig. 30 Relative Drift for Two Studied Systems

- Response Modification Coefficient:** The DCSPs system exhibits a higher response modification coefficient compared to the bracing system, indicating better ductility and seismic performance. Despite both systems reaching the same capacity through capacity equalization via Push-Over analysis, DCSPs offer superior behavior under seismic conditions.
- Stress Distribution and Plastic Behavior:** The DCSPs system shows better stress distribution, with lower and more controlled ultimate stress levels in time history analysis. Furthermore, the plastic behavior of the double corrugated shear wall system surpasses that of traditional bracing systems. This suggests that DCSPs can effectively protect the structural frame members, and due to their ease of installation and architectural advantages, they can function as interchangeable dampers.
- Superior Seismic Performance:** Time history analysis further reveals the advantages of the DCSPs system. It demonstrates greater structural capacity during earthquakes, higher energy absorption, and more significant relative drift, coupled with superior plastic behavior. These characteristics introduce the system as both stiff and resistant to damage while also being ductile and flexible within the elastic range. Thus, DCSPs emerge as an excellent candidate for seismic reinforcement.

Acknowledgments

The research described in this paper was financially supported by the Natural Science Foundation.

References

- Ali, B., Rotimi, A., Tovi, S., Goodchild, C. and Rizzuto, J. (2017), "Evaluation of the influence of creep and shrinkage determinants on column shortening in mid-rise buildings", *Adv. Concrete Constr., Int. J.*, **5**(2), 155-171. <https://doi.org/10.12989/acc.2017.5.2.155>
- American Society of Civil Engineers (2022), "Minimum design loads and associated criteria for buildings and other structures." <https://doi.org/10.1061/9780784414248>
- ANSI/AISC 360-16 (2016), Specification for structural steel buildings, an American National Standard, An American National Standard, Chicago, IL, USA.
- Baboli Nezhadi, E., Labibzadeh, M., Hosseinlou, F. and Khayat, M. (2024), "Machine learning-based design of double corrugated steel plate shear walls", *Int. J. Struct. Integr.*, **15**(6), 1216-1248. <https://doi.org/10.1108/IJSI-09-2024-0152>
- Berman, J.W., Celik, O.C. and Bruneau, M. (2005), "Comparing hysteretic behavior of light-gauge steel plate shear walls and braced frames", *Eng. Struct.*, **27**, 475-485. <https://doi.org/10.1016/j.engstruct.2004.11.007>
- Building Seismic Safety Council (BSSC) (2003), NEHRP Recommended Provisions for Seismic Regulations for New Buildings and Other Structures (FEMA 450), Part 1 338.
- Chao, D., Yi, R., Zi-Qin, J. and Yan, W. (2024), "Lateral resistant behavior of grid-reinforced steel corrugated shear walls", *J. Struct. Eng.*, **150**, p. 4024047.

- <https://doi.org/10.1061/JSENDH.STENG-12285>
Dadmanesh, M. and Mofid, M. (2024), "On the probabilistic seismic damage assessment of trapezoidally corrugated steel plate shear walls", *Results Eng.*, **24**, p. 102971.
<https://doi.org/10.1016/j.rineng.2024.102971>
- Dai, X.M., Ding, Y., Zong, L., Deng, E.F., Lou, N. and Chen, Y. (2018), "Experimental study on seismic behavior of steel strip reinforced CSPSWs in modular building structures", *J. Constr. Steel Res.*, **151**, 228-237.
<https://doi.org/10.1016/j.jcsr.2018.09.022>
- Deng, R., Yang, J.D., Wang, Y.H., Li, Q.Q. and Tan, J.K. (2022), "Cyclic shear performance of built-up double-corrugated steel plate shear walls: Experiment and simulation", *Thin-Walled Struct.*, **181**, p. 110077.
<https://doi.org/10.1016/j.tws.2022.110077>
- Deng, R., Yang, J.D., Gao, Y., Wang, Y.H. and Li, Q.Q. (2023), "Behaviour of double-corrugated steel plates under cyclic in-plane shear loading: An experimental study", *Eng. Struct.*, **276**, p. 115327. <https://doi.org/10.1016/j.engstruct.2022.115327>
- Dey, M. and Alam, M.S. (2024), "Performance based plastic design of friction damped RC building", *Adv. Concrete Constr., Int. J.*, **17**(4), 221-232.
<https://doi.org/10.12989/acc.2024.17.4.221>
- Ouzandja, D., Messaad, M., Berrabah, A.T. and Ouzandja, T. (2025), "3D seismic response of concrete gravity dams considering effect of dam-foundation interface behavior", *Adv. Concrete Constr., Int. J.*, **19**(2), 103-112.
<https://doi.org/10.12989/acc.2025.19.2.103>
- Dou, C., Xie, C., Wang, Y. and Yang, N. (2023), "Cyclic loading test and lateral resistant behavior of flat-corrugated steel plate shear walls", *J. Build. Eng.*, **66**, p. 105831.
<https://doi.org/10.1016/j.jobte.2023.105831>
- Dou, C., Zhang, J., Lan, T., Wang, D. and Zhang, G. (2025), "Elastic shear buckling analysis of infill panels in trapezoidal corrugated plate shear walls", *Thin-Walled Struct.*, **215**, p. 113452. <https://doi.org/10.1016/j.tws.2025.113452>
- Etedali, S., Akbari, M. and Seifi, M. (2019), "MOCS-based optimum design of TMD and FTMD for tall buildings under near-field earthquakes including SSI effects", *Soil Dyn. Earthq. Eng.*, **119**, 36-50. <https://doi.org/10.1016/j.soildyn.2018.12.027>
- Federal Emergency Management Agency (2003), NEHRP recommended provisions for seismic regulations for new buildings and other structures (FEMA 450)."
- Ghodratian-Kashan, S.M. and Maleki, S. (2021), "Cyclic Performance of Corrugated Steel Plate Shear Walls with Beam-Only-Connected Infill Plates", *Adv. Civil Eng.*, **2021**, p. 5542613. <https://doi.org/10.1155/2021/5542613>
- Ghodratian-Kashan, S.M. and Maleki, S. (2022), "Experimental investigation of double corrugated steel plate shear walls", *J. Constr. Steel Res.*, **190**, p. 107138.
<https://doi.org/10.1016/j.jcsr.2022.107138>
- Guo, F., Zhang, Y., Nie, X., Yu, Y., Hu, S., Wei, B. and Jiang, L. (2023), "Effect of openings on lateral behaviors of corrugated plate module walls and high-rise modular buildings", *Thin-Walled Struct.*, **185**, p. 110584.
<https://doi.org/10.1016/j.tws.2023.110584>
- Habibi, A.R., Samadi, M. and Izadpanah, M. (2020), "Practical relations to quantify the amount of damage of SWRCFs using pushover analysis", *Adv. Concrete Constr., Int. J.*, **10**(3), 271-278. <https://doi.org/10.12989/acc.2020.10.3.271>
- Jing, W., Wang, Q., Xing, S., Cheng, X. and Song, Y. (2023), "Control measures of collapse-pounding dynamic responses of adjacent structures under earthquake action", *Soil Dyn. Earthq. Eng.*, **165**, p. 107715.
<https://doi.org/10.1016/j.soildyn.2022.107715>
- Komarizadehasl, S. and Khanmohammadi, M. (2021), "Novel plastic hinge modification factors for damaged RC shear walls with bending performance", *Adv. Concrete Constr., Int. J.*, **12**(4), 355-365.
<https://doi.org/10.12989/acc.2021.12.4.355>
- Li, W., Zha, X. and Yu, J. (2025), "Unified calculation method for load-bearing capacity of corrugated steel shear walls under complex stresses", *Eng. Struct.*, **329**, p. 119811.
<https://doi.org/10.1016/j.engstruct.2025.119811>
- Noruzi, A.H. and Jalaeefar, A. (2024), "Effect of corrugated plate arrangements on the performance of steel shear wall frames", *Structures*, **66**, p. 106871.
<https://doi.org/10.1016/j.istruc.2024.106871>
- Paulay, T. and Priestley, M.J.N. (1992), "Principles of Member Design", Seismic Design of Reinforced Concrete and Masonry Buildings, Chapter 3; Vol. 768, pp. 95-157.
- Rojahn, C., Whittaker, A., Hart, G., Bertero, V., Brandow, G., Freeman, S., Hall, W. and Reaveley, L. (1995), ATC-19 Structural response modification factor; Applied Technology Council, Redwood City, CA, USA.
- Song, E.S. and Kim, J.Y. (2020), "Analytical correction of vertical shortening based on measured data in a RC high-rise building", *Adv. Concrete Constr., Int. J.*, **10**(6), 527-536.
<https://doi.org/10.12989/acc.2020.10.6.527>
- Song, E.S. and Kim, J.Y. (2022), "Effects of analytical correction methods based on measurement results for column shortening", *Adv. Concrete Constr., Int. J.*, **14**(4), 253-267.
<https://doi.org/10.12989/acc.2022.14.1.253>
- Tong, J.Z., Guo, Y.L. and Zuo, J.Q. (2018), "Elastic buckling and load-resistant behaviors of double-corrugated-plate shear walls under pure in-plane shear loads", *Thin-Walled Struct.*, **130**, 593-612. <https://doi.org/10.1016/j.tws.2018.06.021>
- Tong, J.Z., Guo, Y.L., Zuo, J.Q. and Gao, J.K. (2020a), "Experimental and numerical study on shear resistant behavior of double-corrugated-plate shear walls", *Thin-Walled Struct.*, **147**, p. 106485. <https://doi.org/10.1016/j.tws.2019.106485>
- Tong, J.Z., Guo, Y.L. and Pan, W.H. (2020b), "Ultimate shear resistance and post-ultimate behavior of double-corrugated-plate shear walls", *J. Constr. Steel Res.*, **165**, p. 105895.
<https://doi.org/10.1016/j.jcsr.2019.105895>
- Tong, J.Z., Guo, Y.L., Zuo, J.Q. and Gao, J.K. (2020c), "Experimental and numerical study on shear resistant behavior of double-corrugated-plate shear walls", *Thin-Walled Struct.*, **147**, p. 106485. <https://doi.org/10.1016/j.tws.2019.106485>
- Tong, J.Z., Wu, R.M., Xu, Z.Y. and Guo, Y.L. (2023), "Subassemblage tests on seismic behavior of double-corrugated-plate shear walls", *Eng. Struct.*, **276**, p. 115341.
<https://doi.org/10.1016/j.engstruct.2022.115341>
- Vaziri, E., Gholami, M. and Gorji Azandariani, M. (2021), "The wall-frame interaction effect in corrugated steel plate shear walls systems", *Int. J. Steel Struct.*, **21**, 1680-1697.
<https://doi.org/10.1007/s13296-021-00529-3>
- Wang, W., Wang, Y. and Lu, Z. (2018), "Experimental study on seismic behavior of steel plate reinforced concrete composite shear wall", *Eng. Struct.*, **160**, 281-292.
<https://doi.org/10.1016/j.engstruct.2018.01.050>
- Wen, C.B., Zhu, B.L., Sun, H.J., Guo, Y.L., Zheng, W.J. and Deng, L.L. (2024), "Global stability design of double corrugated steel plate shear walls under combined shear and compression loads", *Thin-Walled Struct.*, **199**, p. 111789.
<https://doi.org/10.1016/j.tws.2024.111789>
- Yang, S., Jin, S. and Wang, Q. (2025), "Modular corrugated steel plate shear wall: The relationship of matching with boundary column in terms of stiffness and strength", *J. Constr. Steel Res.*, **227**, p. 109341. <https://doi.org/10.1016/j.jcsr.2025.109341>
- Zeynalian, M. and Ronagh, H.R. (2011), "A numerical study on seismic characteristics of knee-braced cold formed steel shear walls", *Thin-Walled Struct.*, **49**, 1517-1525.
<https://doi.org/10.1016/j.tws.2011.07.012>

- Zhang, H. and Chen, Z. (2021), "Comparison and prediction of seismic performance for shear walls composed with fiber reinforced concrete", *Adv. Concrete Constr., Int. J.*, **11**(2), 111-126. <https://doi.org/10.12989/acc.2021.11.2.111>
- Zhang, X., Zhang, X., Liu, W., Li, Z., Zhang, X. and Zhou, Y. (2021), "Experimental study on shear, tensile, and compression behaviors of composite insulated concrete sandwich wall", *Adv. Concrete Constr., Int. J.*, **11**(1), 33-43. <https://doi.org/10.12989/acc.2021.11.1.033>